ELSEVIER

Journal of Organometallic Chemistry 551 (1998) 27–36

Journal of Organometallic Chemistry

Carborane complexes of ruthenium: studies on the chemistry of the $Ru(CO)_2(\eta^5\text{-}7,8\text{-}Me_2\text{-}7,8\text{-}C_2B_9H_9)$ fragment and the X-ray crystal structure of $[NEt_4][Ru_2(\mu\text{-}Tl)(CO)_4(\eta^5\text{-}7,8\text{-}Me_2\text{-}7,8\text{-}C_2B_9H_9)_2]$ [1,2]

John C. Jeffery [a], Paul A. Jelliss [b], Yi-Hsien Liao [b], F. Gordon A. Stone [b,*]

[a] *School of Chemistry, University of Bristol, Bristol BS8 1TS, UK*
[b] *Department of Chemistry, Baylor University, Waco, TX 76798-7348, USA*

Received 22 April 1997; revised 8 June 1997; accepted 8 June 1997

Abstract

Reactions between $Tl[closo\text{-}1,2\text{-}Me_2\text{-}3,1,2\text{-}TlC_2B_9H_9]$ and $[RuBr(CO)_3(\eta^3\text{-}C_3H_5)]$ in tetrahydrofuran (THF) affords mixtures of the compounds $[Ru(CO)_3(\eta^5\text{-}7,8\text{-}Me_2\text{-}7,8\text{-}C_2B_9H_9)]$ (**1b**) and $Tl[Ru_2(\mu\text{-}Tl)(CO)_4(\eta^5\text{-}7,8\text{-}Me_2\text{-}7,8\text{-}C_2B_9H_9)_2]$ (**2a**) in a ratio 2:3. Treatment of the mixtures with $[NEt_4]I$ followed by I_2 produces $[NEt_4][RuI(CO)_2(\eta^5\text{-}7,8\text{-}Me_2\text{-}7,8\text{-}C_2B_9H_9)]$ (**3b**) as the only product. Complex **2a**, isolated as the $[NEt_4]^+$ salt **2b**, was the subject of a single-crystal X-ray diffraction analysis. The compound crystallises in the orthorhombic space group *Pbcn* [$a = 23.164(2)$, $b = 13.780(2)$, $c = 11.560(6)$ Å]. The structure of the anion consists of two $Ru(CO)_2(\eta^5\text{-}7,8\text{-}Me_2\text{-}7,8\text{-}C_2B_9H_9)$ fragments linked together via a thallium atom, with the complex carrying an overall uninegative charge. The synthon $[Ru(THF)(CO)_2(\eta^5\text{-}7,8\text{-}Me_2\text{-}7,8\text{-}C_2B_9H_9)]$ (**4b**) is readily generated from **3b** by the addition of $AgBF_4$ in THF. The same procedure in MeCN produces the complex $[Ru(NCMe)(CO)_2(\eta^5\text{-}7,8\text{-}Me_2\text{-}7,8\text{-}C_2B_9H_9)]$ (**4c**). The removal of THF from **4b** in vacuo gave the 16-electron complex $[Ru(CO)_2(\eta^5\text{-}7,8\text{-}Me_2\text{-}7,8\text{-}C_2B_9H_9)]$ and a polymeric material postulated to be $[Ru(CO)_2(\eta^5\text{-}7,8\text{-}Me_2\text{-}7,8\text{-}C_2B_9H_9)]_n$. Reaction of solutions of **4b** in CH_2Cl_2 with 2-electron donor ligands yields the complexes $[Ru(L)(CO)_2(\eta^5\text{-}7,8\text{-}Me_2\text{-}7,8\text{-}C_2B_9H_9)]$ (**4d**, L = PPh_3; **4e**, L = $CNBu^t$; **4f**, L = NC_5H_5). Addition of alkenes and alkynes to CH_2Cl_2 solutions of **4b** did not give stable η^2-adducts, but the species $[Ru(CO)_2(\eta^5\text{-}7,8\text{-}Me_2\text{-}7,8\text{-}C_2B_9H_9)]$ was observed in these reactions. The complex $[Ru(CO)_2(\eta^2,\eta^5\text{-}7,8\text{-}Me_2\text{-}10\text{-}C(H)=C(H)SiMe_3\text{-}7,8\text{-}C_2B_9H_9)]$ (**5a**) was isolated from the reaction between **4b** and $Me_3SiC{\equiv}CH$. The IR and NMR spectra of the new compounds are reported. © 1998 Elsevier Science S.A.

Keywords: Metallacarborane; Ruthenium; Carbonyl

1. Introduction

We have thoroughly investigated the chemistry of the fragment $Ru(CO)_2(\eta^5\text{-}7,8\text{-}C_2B_9H_{11})$ and found it yields a plethora of novel compounds upon reaction with both organic and organometallic reagents [1–3]. Previous work has often led us to observe that the replacement of the CH groups on the carborane ligand by CMe groups provides an interesting variant in such reactions of metallacarborane compounds. Therefore, the next logical step in our investigation of the reactivity of ruthenacarborane complexes was to examine the behaviour of the $Ru(CO)_2(\eta^5\text{-}7,8\text{-}Me_2\text{-}7,8\text{-}C_2B_9H_9)$ moiety. Indeed, reactions of the species $[Ru(THF)(CO)_3(\eta^5\text{-}7,8\text{-}Me_2\text{-}7,8\text{-}C_2B_9H_9)]$ with tungsten– and molybdenum–alkylidynes have produced some remarkable results [3]. We also wished to study reactions with simple 2-electron donor molecules, for the purpose of comparison with results obtained in the $Ru(CO)_2(\eta^5\text{-}7,8\text{-}C_2B_9H_{11})$ work.

2. Results and discussion

The synthetic route to the reactive synthon $[Ru(THF)(CO)_2(\eta^5\text{-}7,8\text{-}C_2B_9H_{11})]$ (**4a**) is displayed in Scheme 1.The first step involves the reaction of

* Corresponding author.

[1] This paper is dedicated to Professor P.M. Maitlis FRS on the occasion of his 65th birthday.

[2] The compounds described in this paper have a ruthenium atom incorporated into a *closo*-1,2-carba-3-ruthenadodecaborane structure. However, to avoid a complicated nomenclature for the complexes reported, and to relate them to the many known ruthenium species with η^5-coordinated cyclopentadienyl ligands, we treat the cages as *nido*-11-vertex ligands with numbering as for an icosahedron from which the twelfth vertex has been removed.

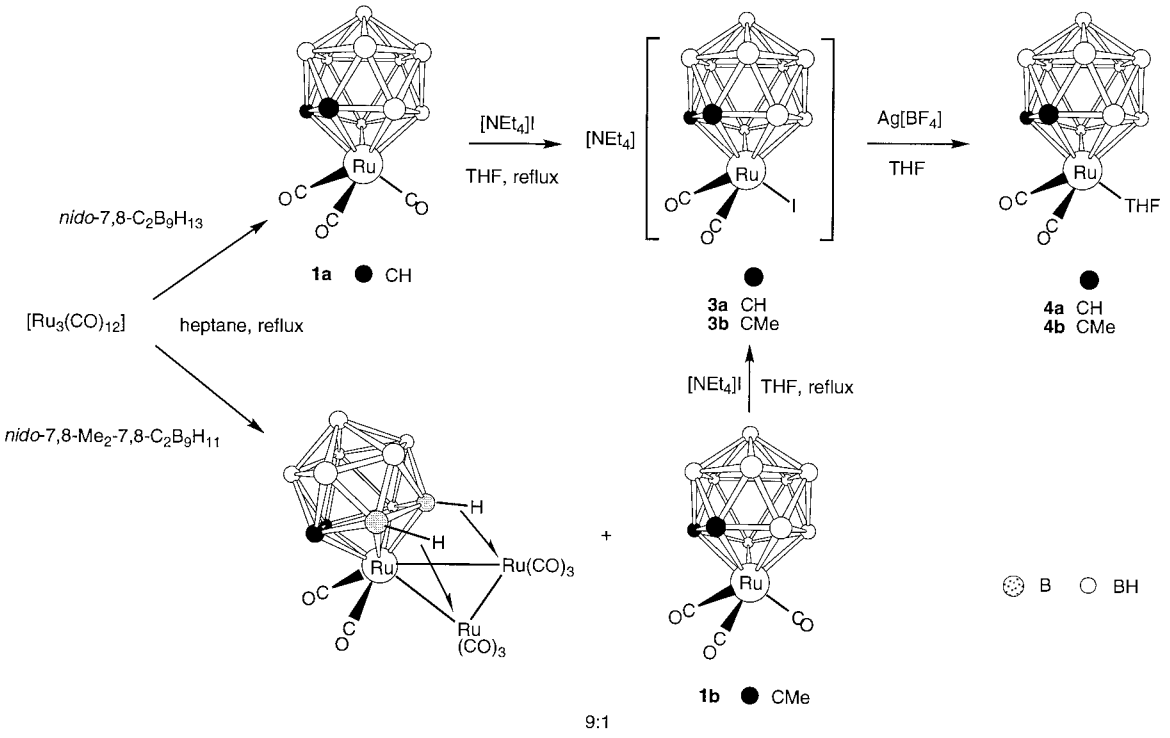

Scheme 1. Original reaction pathway to the synthon **4b.**

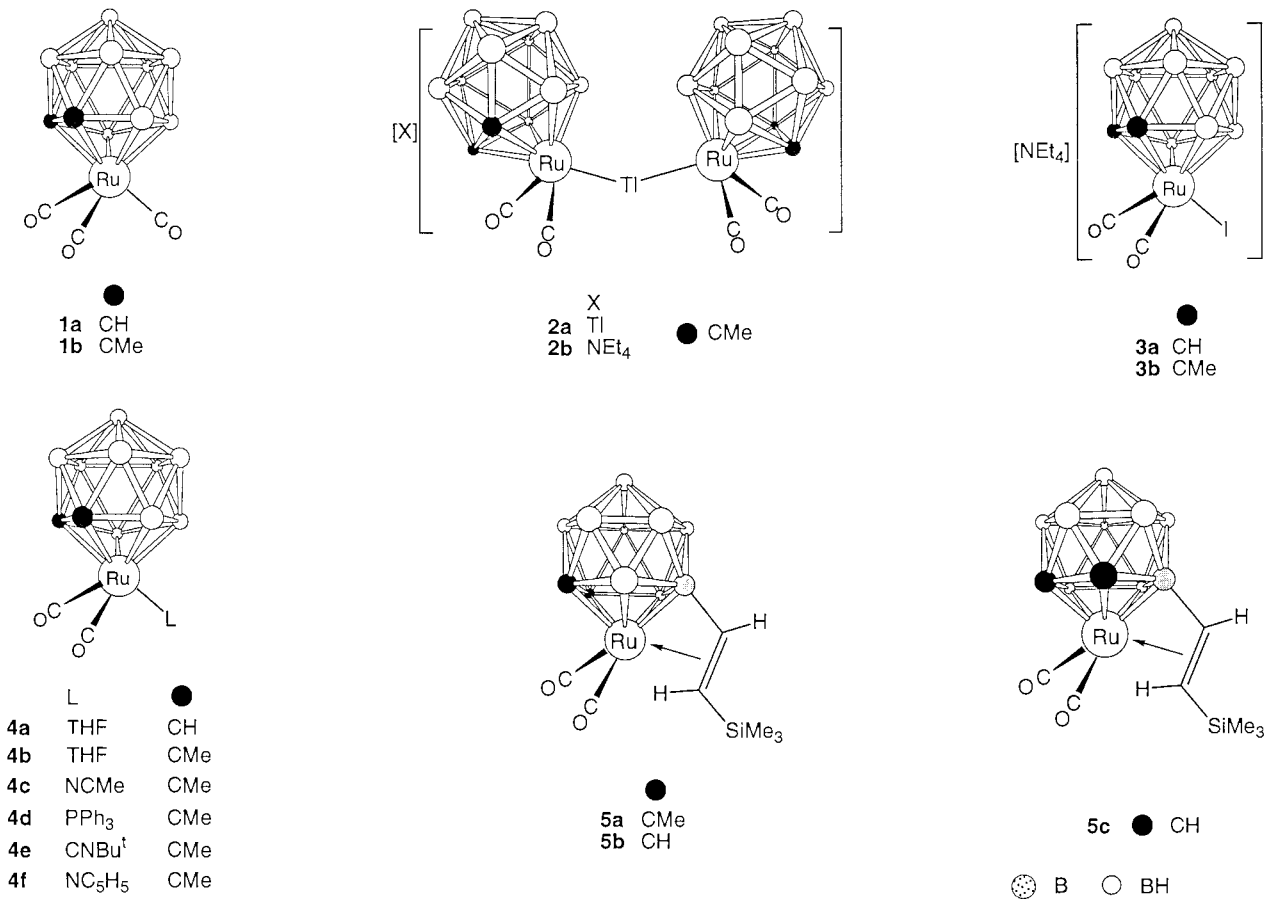

$[Ru_3(CO)_{12}]$ with *nido*-7,8-$C_2B_9H_{13}$ in refluxing heptane to give $[Ru(CO)_3(\eta^5\text{-}7,8\text{-}C_2B_9H_{11})]$ (**1a**), formed as the only product and in good yield [1]. When repeating this methodology using *nido*-7,8-Me_2-7,8-$C_2B_9H_{11}$, a mixture of the trinuclear metal complex $[Ru_3(CO)_8(\eta^5\text{-}7,8\text{-}Me_2\text{-}7,8\text{-}C_2B_9H_9)]$ and the desired mononuclear complex $[Ru(CO)_3(\eta^5\text{-}7,8\text{-}Me_2\text{-}7,8\text{-}C_2B_9H_9)]$ (**1b**) was formed in ratio 9:1 (Scheme 1) [4]. Thus, this method is rendered impractical for the purpose of producing **1b** as a precursor to other complexes, even though the two reaction products are readily separated by column chromatography. Our initial studies of reactions of **1b** with alkylidyne–molybdenum and –tungsten complexes did, however, rely on obtaining the mononuclear species by this route [3].

Further research revealed that the reaction of Tl[*closo*-1,2-Me_2-3,1,2-$TlC_2B_9H_9$] with $[RuBr(CO)_3(\eta^3\text{-}C_3H_5)]$ produced a mixture of two compounds. The major component, $Tl[Ru_2(\mu\text{-}Tl)(CO)_4(\eta^5\text{-}7,8\text{-}Me_2\text{-}7,8\text{-}C_2B_9H_9)_2]$ (**2a**) (60% mol ratio), was isolated as the $[NEt_4]^+$ salt (**2b**) after addition of $[NEt_4]Cl$ and separation from $[Ru(CO)_3(\eta^5\text{-}7,8\text{-}Me_2\text{-}7,8\text{-}C_2B_9H_9)]$ (**1b**). The NMR data for **2b** will be discussed after the results of an X-ray diffraction study on a single crystal of the salt are presented. Selected bond distances and angles are listed in Table 1 and the structure is shown in Fig. 1.

The presence of the bridging thallium atom would not have been detected without the structure determination. The anion consists of two $[Ru(CO)_2(\eta^5\text{-}7,8\text{-}Me_2\text{-}7,8\text{-}C_2B_9H_9)]$ units linked together by the atom Tl(1) and with the ruthenium-cage units twisted relative to each other. The Tl(1)–Ru(1) [and Tl(1)–Ru(1A)] bond distance [2.5995(4) Å] is unusually short and may be compared with the Tl–Ru distances in the compound

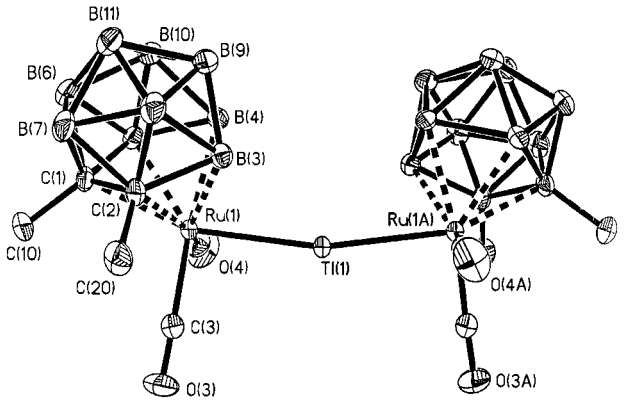

Fig. 1. Structure of the anion of $[NEt_4][Ru_2(\mu\text{-}Tl)(CO)_4(\eta^5\text{-}7,8\text{-}Me_2\text{-}7,8\text{-}C_2B_9H_9)_2]$ (**2b**), showing the crystallographic labeling scheme. Hydrogen atoms are omitted for clarity and thermal ellipsoids are shown at the 40% probability level.

$[AsPh_4][\{Ru_6C(CO)_{16}\}_2(\mu_4\text{-}Tl)]$ [2.780(3) and 2.864(2) Å] [5]. If bonding in complex **2b** were considered to involve purely ionic interactions between two $Ru(II)^{1-}$ fragments and a $Tl(I)^{1+}$ ion, as has been postulated for previously synthesised thallium(I)-transition metal complexes, longer Tl–Ru interactions in **2b** might have been expected. It has been proposed that in the complex salt $[Ir_2(\mu\text{-}Tl)\{\mu\text{-}(PPh_2CH_2)_2AsPh\}_2(Cl)_2(CO)_2][NO_3]$ [6], a significant covalent interaction between the filled $5d_{z^2}$ orbitals and empty $6p_z$ on the iridium atoms with the filled 6s and empty $6p_y$ and $6p_z$ orbitals on the thallium atom leads to enhanced stability of the system and thus to short Tl–Ir bonds. A similar situation can be envisaged in **2b**, possibly utilizing filled 4d and empty 5p orbitals of suitable symmetry on the ruthenium atoms with the filled 6s and empty 6p orbitals on the thallium atom. It should be noted that the Ir–Tl–Ir bond angle in $[Ir_2(\mu\text{-}Tl)\{\mu\text{-}(PPh_2CH_2)_2AsPh\}_2(Cl)_2(CO)_2][NO_3]$ is

Table 1
Selected internuclear distances (Å) and angles (deg) for **2b** with estimated standard deviations in parentheses

Tl(1)–Ru(1)	2.5994(4)	Ru(1)–C(4)	1.857(4)	Ru(1)–C(3)	1.911(4)	Ru(1)–B(5)	2.244(4)
Ru(1)–C(1)	2.270(3)	Ru(1)–C(2)	2.276(4)	Ru(1)–B(3)	2.284(4)	Ru(1)–B(4)	2.294(4)
C(1)–C(10)	1.532(5)	C(1)–C(2)	1.682(5)	C(1)–B(6)	1.715(6)	C(1)–B(5)	1.723(5)
C(1)–B(7)	1.733(6)	C(2)–C(20)	1.528(5)	C(2)–B(8)	1.708(6)	C(2)–B(3)	1.713(5)
C(2)–B(7)	1.730(6)	B(3)–B(8)	1.765(6)	B(3)–B(9)	1.769(6)	B(3)–B(4)	1.829(6)
B(4)–B(9)	1.784(6)	B(4)–B(10)	1.790(6)	B(4)–B(5)	1.829(6)	B(5)–B(10)	1.789(6)
B(5)–B(6)	1.793(6)	B(6)–B(7)	1.750(7)	B(6)–B(11)	1.769(7)	B(6)–B(10)	1.765(6)
B(7)–B(8)	1.751(7)	B(7)–B(11)	1.757(7)	B(8)–B(9)	1.760(7)	B(8)–B(11)	1.762(7)
B(9)–B(11)	1.766(6)	B(9)–B(10)	1.782(7)	B(10)–B(11)	1.777(7)	C(3)–O(3)	1.136(6)
C(4)–O(4)	1.154(5)						
Ru(1)–Tl(1)–Ru(1A)	165.67(2)	C(4)–Ru(1)–C(3)	89.5(2)	C(4)–Ru(1)–B(5)	86.5(2)		
C(3)–Ru(1)–B(5)	140.5(2)	C(4)–Ru(1)–C(1)	115.5(2)	C(3)–Ru(1)–C(1)	104.0(2)		
B(5)–Ru(1)–C(1)	44.88(14)	C(4)–Ru(1)–C(2)	159.0(2)	C(3)–Ru(1)–C(2)	96.2(2)		
B(5)–Ru(1)–C(2)	76.23(14)	C(1)–Ru(1)–C(2)	43.44(13)	C(4)–Ru(1)–B(3)	144.3(2)		
C(3)–Ru(1)–B(3)	121.8(2)	B(5)–Ru(1)–B(3)	79.4(2)	C(1)–Ru(1)–B(3)	75.93(14)		
C(2)–Ru(1)–B(3)	44.12(13)	C(4)–Ru(1)–B(4)	100.1(2)	C(3)–Ru(1)–B(4)	168.5(2)		
B(5)–Ru(1)–B(4)	47.5(2)	C(1)–Ru(1)–B(4)	77.63(14)	C(2)–Ru(1)–B(4)	77.07(14)		
B(3)–Ru(1)–B(4)	47.10(14)	C(4)–Ru(1)–Tl(1)	88.37(13)	C(3)–Ru(1)–Tl(1)	90.95(12)		
B(5)–Ru(1)–Tl(1)	128.17(11)	C(1)–Ru(1)–Tl(1)	151.41(10)	C(2)–Ru(1)–Tl(1)	111.68(9)		
B(3)–Ru(1)–Tl(1)	75.48(10)	B(4)–Ru(1)–Tl(1)	83.09(10)	O(3)–C(3)–Ru(1)	178.3(4)		
O(4)–C(4)–Ru(1)	176.5(4)						

distinctly bent at 139.4(1)°, but in this complex the iridiums are constrained within two near-parallel square-planar systems. In complex **2b**, the Ru(1)–Tl(1)–Ru(1A) angle is less deviated from linearity at 165.67(2)°.

The analytical and NMR data for complex **2b** are given in Tables 2 and 3. The IR spectrum showed three terminal ν_{max}(CO) absorption bands at 2014, 1992, and 1954 cm^{-1}. In the ^1H NMR spectrum, one signal is observed for the cage methyl protons at δ 2.21, while in the $^{13}C\{^1H\}$ NMR spectrum, two signals are noted at δ 68.8 and 32.8 for the cage *C*Me and C*Me* carbon nuclei, respectively, the former being characteristically broad. A single very broad peak due to the carbonyl ligands was observed in the range δ 195–200. A variable temperature $^{13}C\{^1H\}$ NMR experiment revealed that this peak sharpened up somewhat in spectra measured down to −55°C. It is suggested that the broadness of the peak at ambient temperature may be due to partial dissociation of the anion of **2b** in solution into $[RuTl(CO)_2(\eta^5\text{-}7,8\text{-}Me_2\text{-}7,8\text{-}C_2B_9H_9)]^-$ and a neutral 16-electron species $[Ru(CO)_2(\eta^5\text{-}7,8\text{-}Me_2\text{-}7,8\text{-}C_2B_9H_9)]$, the existence of the latter having basis in chemistry discussed shortly. It was noted that the signal due to the cage carbon *C*Me nuclei at −55°C was also considerably sharper than in the corresponding room-temperature spectrum. The C*Me* carbon and proton nuclei showed less enhanced signal sharpening in the low-temperature spectra. To account for the broadness in the spectra at ambient temperatures, the dissociation–reassociation process must be occurring at or near the NMR time scale. Unfortunately it was not possible to study this phenomenon at elevated temperatures because of the absence of suitable NMR solvents in which the compound is soluble. The room-temperature $^{11}B\{^1H\}$ NMR spectrum showed a pattern of broad signals (1:2:3:1:2) consistent with two equivalent *nido*-C_2B_9 cages with a mirror plane of symmetry.

Returning to the synthesis of **2a**, it will be recalled that this salt is formed with complex **1b** in ratio ca. 3:2. If this mixture is treated with $[NEt_4]I$ in refluxing tetrahydrofuran (THF), **1b** is converted to $[NEt_4][RuI(CO)_2(\eta^5\text{-}7,8\text{-}Me_2\text{-}7,8\text{-}C_2B_9H_9)]$ (**3b**), while **2a** is converted to **2b**, as assessed by IR spectroscopy. At this point, the mixture is cooled to 0°C and treated very carefully with I_2 to convert **2b** to **3b** which, in this manner, is formed as the sole product and in high yield. Hence, a one-pot synthesis of the useful reagent **3b** from $Tl[closo\text{-}1,2\text{-}Me_2\text{-}3,1,2\text{-}TlC_2B_9H_9]$ and $[RuBr(CO)_3(\eta^3\text{-}C_3H_5)]$ has become available (Scheme 2). The mechanism of the reaction of **2b** with I_2 is unclear, but may involve the intermediacy of the dissociation fragments $[RuTl(CO)_2(\eta^5\text{-}7,8\text{-}Me_2\text{-}7,8\text{-}C_2B_9H_9)]^-$ and $[Ru(CO)_2(\eta^5\text{-}7,8\text{-}Me_2\text{-}7,8\text{-}C_2B_9H_9)]$ mentioned above.

Complex **3b** is a new compound and was characterised by standard spectroscopic and analytical techniques; data are listed in Tables 2 and 3. The IR spectrum revealed two terminal CO bands at 2034 and 1984 cm^{-1}, as expected. In the ^1H NMR spectrum, a singlet resonance was observed for the cage methyl groups at δ 2.34, while signals in the $^{13}C\{^1H\}$ NMR spectrum at δ 198.4, 71.2, and 33.6 confirmed the presence of the equivalent carbonyl ligands, and the cage carbon and cage methyl nuclei, respectively.

The treatment of the salt **3b** with $AgBF_4$ in THF produces the solvent adduct $[Ru(THF)(CO)_2(\eta^5\text{-}7,8\text{-}Me_2\text{-}7,8\text{-}C_2B_9H_9)]$ (**4b**), an analog of the previously studied complex **4a** [1]. The IR spectrum of **4b** in THF shows strong ν_{max}(CO) absorptions at 2044 and 1994

Table 2
Analytical and physical data

Compound[a]	ν_{max}(CO)[b] (cm^{-1})	Yield(%)	Analysis (%)[c]		
			C	H	N
$[NEt_4][Ru_2(\mu\text{-}Tl)(CO)_4(\eta^5\text{-}7,8\text{-}Me_2\text{-}7,8\text{-}C_2B_9H_9)_2]$ (**2b**)	2014 m, 1992 s, 1995 m	33	24.4 (24.8)	5.2 (5.2)	1.4 (1.4)
$[NEt_4][RuI(CO)_2(\eta^5\text{-}7,8\text{-}Me_2\text{-}7,8\text{-}C_2B_9H_9)]$ (**3b**)	2034 s, 1984 s	97	28.8 (29.3)	5.8 (6.1)	2.0 (2.4)
$[Ru(THF)(CO)_2(\eta^5\text{-}7,8\text{-}Me_2\text{-}7,8\text{-}C_2B_9H_9)]$ (**4b**)[d]	2044 s, 1994 s[e]	62			
$[Ru(NCMe)(CO)_2(\eta^5\text{-}7,8\text{-}Me_2\text{-}7,8\text{-}C_2B_9H_9)]$ (**4c**)	2060 s, 2014 s	78	26.9 (26.8)	5.1 (5.0)	3.9 (3.9)
$[Ru(PPh_3)(CO)_2(\eta^5\text{-}7,8\text{-}Me_2\text{-}7,8\text{-}C_2B_9H_9)]$ (**4d**)	2040 s, 1990 s	51	49.3 (49.7)	5.2 (5.2)	
$[Ru(CNBu^t)(CO)_2(\eta^5\text{-}7,8\text{-}Me_2\text{-}7,8\text{-}C_2B_9H_9)]$ (**4e**)	2066 s, 2022 s[f]	85	32.7 (33.0)	6.2 (6.0)	3.4 (3.5)
$[Ru(NC_5H_5)(CO)_2(\eta^5\text{-}7,8\text{-}Me_2\text{-}7,8\text{-}C_2B_9H_9)]$ (**4f**)	2050 s, 1998 s	87	33.2 (33.3)	5.1 (5.1)	3.5 (3.5)
$[Ru(CO)_2\{\eta^2,\eta^5\text{-}7,8\text{-}Me_2\text{-}10\text{-}C(H)=C(H)SiMe_3\text{-}7,8\text{-}C_2B_9H_8\}]$ (**5a**)	2042 s, 1994 s	21	31.9 (31.8)	6.1 (6.1)	

[a] All complexes are yellow in colour except **3b**, which is red.
[b] Measured in CH_2Cl_2 unless otherwise stated. A medium-intensity broad band observed at ca. 2550 cm^{-1} in the spectra of all the compounds is due to B–H absorptions.
[c] Calculated values are given in parentheses.
[d] When samples are dried in vacuo, THF is lost with some decomposition: microanalysis not available. While it was not possible to obtain the 16-electron complex $[Ru(CO)_2(\eta^5\text{-}7,8\text{-}Me_2\text{-}7,8\text{-}C_2B_9H_9)]$ in sufficient purity for microanalysis, an EI mass spectrum was measured: 318.10 (33% relative peak height, parent molecular ion, calc. 318.02), 290.03 (71% relative peak height, –CO × 1), 262.04 (100% relative peak height, –CO × 2).
[e] Measured in THF solution.
[f] ν_{max}(NC) 2186 cm^{-1}.

Table 3
Hydrogen-1, carbon-13 and boron-11 NMR data[a]

Compound	^{1}H (δ)[b]	^{13}C (δ)[c]	^{11}B (δ)[d]
2b[e]	1.39 [t of t, 12 H, Me, J(HH) = 7, J(NH) = 2], 2.21 (s, 12 H, cage Me), 3.47 [q, 8 H, CH_2, J(HH) = 7]	197.8 (v br, CO), 68.8 (br, cage C), 53.0 (CH_2), 32.8 (cage Me), 7.7 (Me)	−1.2 (1 B), −5.8 (2 B), −9.4 (3 B), −11.7 (1 B), −15.1 (2 B)
3b	1.34 [t of t, 12 H, Me, J(HH) = 7, J(NH) = 2], 2.34 (s, 6 H, cage Me), 3.21 [q, 8 H, CH_2, J(HH) = 7]	198.4 (CO), 71.2 (br, cage C), 53.1 (CH_2), 33.6 (cage Me), 7.8 (Me)	1.1 (1 B), −5.1 (2 B), −9.9 (4 B), −16.4 (2 B)
4b[f]	1.79 (m, 4 H, CH_2), 1.83 (s, 6 H, cage Me), 3.63 (m, 4 H, CH_2O)	196.9 (CO), 79.1 (cage C), 68.0 (CH_2O), 26.1 (cage Me and CH_2)	5.1 (1 B), −4.7 (2 B), −8.6 (2 B), −9.8 (1 B), −13.3 (1 B), −15.4 (2 B)
4c	1.95 (s, 6 H, cage Me), 2.39 (s, 3 H, Me)	194.8 (CO), 121.3 (CN), 76.8 (cage C), 28.5 (cage Me), 4.2 (Me)	5.6 (1 B), −4.5 (2 B), −8.2 (2 B), −9.9 (1 B), −10.9 (1 B), −14.8 (2 B)
4d[g]	2.07 (s, 6 H, cage Me), 7.40 − 7.68 (m, 15 H, Ph)	197.0 [d, CO, J(PC) = 16], 133.9 [d, C^2(Ph), J(PC) = 10], 132.6 [d, C^1(Ph), J(PC) = 53], 131.5 [d, C^4(Ph), J(PC) = 3], 128.9 [d, C^3(Ph), J(PC) = 11], 71.8 (cage C), 31.3 (cage Me)	3.4 (1 B), −2.4 (1 B), −4.0 (2 B), −6.5 (3 B), −12.0 (2 B) 3.4 (1 B), −2.4 (1 B), −4.0 (2 B), −6.5 (3 B), −12.0 (2
4e	1.57 (s, 9 H, Me), 2.16 (s, 6 H, cage Me)	193.7 (CO), 137.2 [t, NC, J(NC) = 20], 74.3 (cage C), 59.9 (CMe_3), 31.9 (cage Me), 30.1 (CMe_3)	5.1 (1 B), −4.5 (2 B), −6.3 (1 B), −7.0 (2 B), −9.2 (1 B), −13.2 (2 B)
4f[e]	1.75 (s, 6 H, cage Me), 7.74(m, 2 H, NC_5H_5), 8.21 (m, 1 H, NC_5H_5), 9.06 (m, 2 H, NC_5H_5)	197.2 (CO), 156.9, 140.8, 128.1 (2C:1C:2C, NC_5H_5), 73.4 (cage C), 27.7 (cage Me)	7.1 (1 B), −2.8 (2B), −5.2 (2 B), −6.7 (2 B), −10.9 (2 B)
5a	0.27 (s, 9 H, $SiMe_3$), 3.76 [d, 1 H, =C(H)$SiMe_3$, J(HH) = 15], 4.94 [d, 1 H, =C(H)B, J(HH) = 15]	196.7, 193.7 (CO), 98.5 [vbr, =C(H)B], 82.7 (cage C), 75.8 [=C(H)$SiMe_3$], 67.5 (cage C), 32.3, 31.4 (cage Me), −0.7 ($SiMe_3$)	19.2 [1 B, BC(H)=C^h], 2.4 (1 B), −2.2 (1 B), −3.5 (1 B), −7.4 (1 B), −9.6 (2 B), −11.3 (1 B), −12.7 (1 B)

[a] Chemical shifts (δ) in ppm, coupling constants (J) in Hz, measurements at ambient temperature in CD_2Cl_2 unless otherwise stated.
[b] Resonances for terminal BH protons occur as broad unresolved signals in the range of δ ca. −2 to 3.
[c] Hydrogen-1 decoupled, chemical shifts are positive to high frequency of $SiMe_4$.
[d] Hydrogen-1 decoupled, chemical shifts are positive to high frequency of $BF_3 \cdot OEt_2$ (external).
[e] Measurements in d^6-acetone.
[f] Measurement in CD_2Cl_2–THF (10:1).
[g] $^{31}P\{^1H\}$ NMR: δ 45.7.
[h] Identified in a fully coupled ^{11}B NMR spectrum.

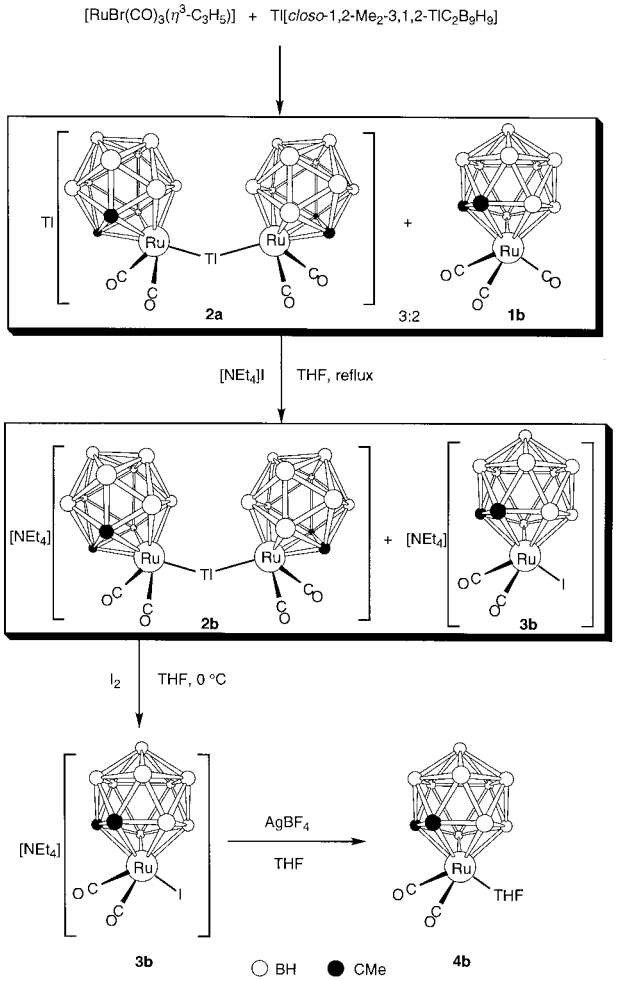

Scheme 2. New one-pot synthesis of the complex **4b**.

cm^{-1}. If THF is removed in vacuo, an orange residue results, which, after drying for at least 24 h in vacuo, shows only limited solubility in CH_2Cl_2. An IR spectrum of the weak solution produced reveals two principal peaks at 2060 and 2014 cm^{-1}. The difference between these frequencies and those for freshly prepared THF solutions of **4b** are too great to be attributed to a 'solvent change' effect. Thus as was observed with **4a** [1], loss of coordinated THF to give a 16-electron complex $[Ru(CO)_2(\eta^5\text{-}7,8\text{-}Me_2\text{-}7,8\text{-}C_2B_9H_9)]$ is believed to occur. Two further weak peaks are also observed in the IR spectrum of CH_2Cl_2 solutions of the orange residue at 2070 and 2026 cm^{-1} and we believe that these may be due to a polymeric species $[Ru(CO)_2(\eta^5\text{-}7,8\text{-}Me_2\text{-}7,8\text{-}C_2B_9H_9)]_n$. Indeed this polymeric compound constitutes the bulk of the insoluble material. A nujol mull IR spectrum of the solid displays bands at 2066 and 2034 cm^{-1}, which are similar to the weaker set of peaks in the spectrum measured on a CH_2Cl_2 solution. A polymeric form of ruthenium carbonyl, $[Ru(CO)_4]_n$, has been isolated by treatment of $Ru_3(CO)_{12}$ solutions under CO with UV irradiation or sunlight [7,8], and its structure has been determined by an X-ray powder diffraction study [8]. Polymeric transition metal carbonyl complexes are few in number, but clearly there is some capacity for ruthenium carbonyl units to undergo this kind of chain aggregation. The nature of the polymeric species $[Ru(CO)_2(\eta^5\text{-}7,8\text{-}Me_2\text{-}7,8\text{-}C_2B_9H_9)]_n$ is unknown. An EI mass spectrum of this orange material clearly shows a parent molecular ion peak for the 16-electron moiety $[Ru(CO)_2(\eta^5\text{-}7,8\text{-}Me_2\text{-}7,8\text{-}C_2B_9H_9)]$ at 318.10, with two further peaks at 290.03 and 262.04 due to molecular ions resulting from loss of one and two CO ligands, respectively, from the parent. There was no mass spectral evidence for any molecular ions with $n > 1$. A ^1H NMR spectrum of the weak solution formed upon addition of CD_2Cl_2 indicated that no THF was present in the sample. An $^{11}B\{^1H\}$ NMR spectrum of the same solution was complex, and contained additional peaks in the range δ −30 to −40, which are almost certainly due to a *nido*-cage species, indicating that some decomposition has occurred. When THF is added to the orange residue, most of the solid is taken up to form a yellow solution, with some unidentified insoluble black material remaining. An IR spectrum of the THF solution, shows it to contain only the adduct **4b**. Hence, to some extent THF dissociation is reversible.

If solutions of complex **4b** generated in THF undergo solvent removal in vacuo, the resulting residue can subsequently be redissolved in CH_2Cl_2, provided the sample has not been evacuated for an extended period of time. Dissolving **4b** in CH_2Cl_2 also has the effect of activating the complex towards reaction with other donor molecules. NMR measurements were made on a sample of complex **4b** dissolved in CD_2Cl_2 with a very small amount of added THF to stabilise the complex. The ^1H NMR spectrum revealed two sets of multiplets at δ 1.79 and 3.63 due to the CH_2 protons of the ligating THF, which may be compared with the corresponding signals in complex **4a** (δ 1.99 and 3.90). Also in the ^1H NMR spectrum of **4b**, a single resonance for the cage CMe groups was observed at δ 1.83. The $^{13}C\{^1H\}$ NMR spectrum showed two resonances for the ligated THF at δ 68.0 and 26.1, with singlet signals observed for the CO, cage *C*Me and C*Me* carbon nuclei at δ 196.9, 79.1, and 26.1, respectively, confirming the presence of a mirror plane containing the Ru atom, the THF oxygen atom and the mid-point of the cage C–C connectivity.

The compound $[Ru(NCMe)(CO)_2(\eta^5\text{-}7,8\text{-}Me_2\text{-}7,8\text{-}C_2B_9H_9)]$ (**4c**), an analog of complex **4b**, was readily prepared by treating the salt **3b** with $AgBF_4$ in MeCN. The IR spectrum showed ν_{max}(CO) stretching bands at 2060 and 2014 cm^{-1}. The NMR spectra revealed resonances for the ligated MeCN molecule at δ 2.39 in the ^1H spectrum and at 121.3 (N*C*Me) and 4.2 (NC*Me*) in the $^{13}C\{^1H\}$ spectrum. The equivalent cage methyl groups also give rise to signals at δ 1.95 (^1H spectrum)

and 28.5 ($^{13}C\{^1H\}$ spectrum), with the cage carbon nuclei showing the usual broad resonance at δ 76.8 in the latter NMR spectrum. The $^{11}B\{^1H\}$ NMR spectrum was as expected (Table 3).

The addition of PPh_3, Bu^tNC, and pyridine to CH_2Cl_2 solutions of reagent **4b** generates the stable complexes $[Ru(L)(CO)_2(\eta^5\text{-}7,8\text{-}Me_2\text{-}7,8\text{-}C_2B_9H_9)]$ (**4d**, L = PPh_3; **4e**, L = $CNBu^t$; **4f**, L = NC_5H_5), respectively, all isolated in good yield after column chromatography. All molecules possess C_s symmetry as evidenced by their $^{11}B\{^1H\}$ NMR spectra (Table 3). Furthermore, the ^1H and $^{13}C\{^1H\}$ NMR spectra of the complexes revealed single resonances for the cage carbon and cage methyl nuclei in addition to single peaks for the CO carbon nuclei (Table 3). The $^{31}P\{^1H\}$ NMR spectrum of **4d** showed the expected singlet for the ligated phosphine at δ 45.7. The spectra of compound **4e** were as expected with a ν_{max}(NC) band in the IR spectrum at 2186 cm^{-1} and the *C*NBu^t nucleus giving rise to a triplet resonance in the $^{13}C\{^1H\}$ NMR spectrum at δ 137.2 [J(NC) = 20 Hz].

The treatment of compound **4a** with alkenes, alkynes and transition metal alkylidynes has proven extremely fruitful [2,3]. Some reactions of complex **4b** with transition metal alkylidynes have also been documented [3], but to date we have not reported reactions of **4b** with simple alkenes and alkynes. A CH_2Cl_2 solution of complex **4b**, when treated with C_7H_{12} (norbornene), did not yield a stable ruthenium–alkene adduct. IR and mass spectral analysis revealed that the fragment $[Ru(CO)_2(\eta^5\text{-}7,8\text{-}Me_2\text{-}7,8\text{-}C_2B_9H_9)]$ had been formed, along with unidentified dark solid, which may be the polymeric $[Ru(CO)_2(\eta^5\text{-}7,8\text{-}Me_2\text{-}7,8\text{-}C_2B_9H_9)]_n$. To our surprise, a similar result was obtained when CH_2Cl_2 solutions of **4b** were treated with one or two equivalents of MeC≡CMe, PhC≡CPh, or Bu^{t}C≡CH, respectively. This is in stark contrast with the reactivity of complex **4a**, which forms stable adducts with alkenes and alkynes. In the corresponding reactions of **4b**, some $[Ru(CO)_2(\eta^5\text{-}7,8\text{-}Me_2\text{-}7,8\text{-}C_2B_9H_9)]$ was detected in all cases. The $^{11}B\{^1H\}$ NMR spectra of the residues from the reactions were complex and indicated that *nido*-cage systems were also present with peaks appearing at $< \delta -30$, and other resonances in these spectra did not show $^1H-^{11}B$ coupling in fully coupled ^{11}B NMR spectra. The treatment of complex **4b** with a very large excess of the alkenes or alkynes still produced intractable mixtures and we have not been able to harness these reactions. Thus, uncontrolled multiple hydroborations of the unsaturated hydrocarbon molecules may have occurred, leading eventually to partial decomposition of the *closo*-3,1,2-RuC_2B_9 cluster. It is, however, possible to report a positive result with one particular alkyne: reaction of a CH_2Cl_2 solution of **4b** with $Me_3SiC{\equiv}CH$ gave a very complicated mixture. Nevertheless, after preparative thin layer chromatography (TLC), material in one of the yellow fractions was characterised as $[Ru(CO)_2(\eta^2,\eta^5\text{-}7,8\text{-}Me_2\text{-}10\text{-}C(H){=}C(H)SiMe_3\text{-}7,8\text{-}C_2B_9H_8)]$ (**5a**).

The ^1H NMR spectrum of compound **5a** showed two sets of doublet signals at δ 3.76 and 4.94 [J(HH) = 15 Hz] corresponding to the *trans* C(H)=C(H) protons. As a result of the asymmetry of the system, two singlets are observed in the ^1H NMR spectrum for the cage methyl groups (δ 2.37 and 2.43) and four signals are observed in the $^{13}C\{^1H\}$ NMR spectrum at δ 67.5 and 82.7 (*C*Me) and at 31.4 and 32.3 (C*Me*). Also in this spectrum, a broad resonance was observed at δ 98.5, and this may be assigned to the vinyl carbon bound to one of the boron atoms in the metal-coordinating $\overline{CCBBB}$ face of the cage. The other vinyl carbon, to which the $SiMe_3$ group is bound, displayed a signal at δ 75.8. The $^{11}B\{^1H\}$ NMR spectrum showed a resonance at δ 19.2, which is attributable to the cage β-boron carrying the η^2-C(H)=C(H)$SiMe_3$ group, with this signal showing as expected no $^1H-^{11}B$ coupling in the fully coupled ^{11}B NMR spectrum. The chemical shift is similar in magnitude to that for the corresponding β-B nucleus in the related complex $[Ru(CO)_2(\eta^2,\eta^5\text{-}10\text{-}C(H){=}C(H)SiMe_3\text{-}7,8\text{-}C_2B_9H_{10})]$ (**5b**) (δ 20.0) [2]. The ^{11}B NMR spectra allow us to distinguish which boron atom in the coordinating face of the cage may be involved in the non-innocent behaviour. Thus the corresponding signal for the compound $[Ru(CO)_2(\eta^2,\eta^5\text{-}9\text{-}C(H){=}C(H)SiMe_3\text{-}7,8\text{-}C_2B_9H_{10})]$ (**5c**), where an α-boron is utilised in the $\overline{CC\mathit{B}BB}$ coordinating ring, occurs at δ 10.2 [2]. Compound **5c** is formed in the same reaction as **5b**, and is readily separated by column chromatography. The employment of the β-boron in compound **5a** is further supported by previous observations that the presence of methyl groups on the cage carbons increases the propensity of the β-B–H bonds to become activated over the α-B–H bonds [9]. However, we cannot rule out the formation of an α-isomer of compound **5a**, which may be present in the remainder of the intractable mixture.

3. Conclusion

The formation of the salt **2a** from Tl[*closo*-1,2-Me_2-3,1,2-$TlC_2B_9H_9$] and $[RuBr(CO)_3(\eta^3\text{-}C_3H_5)]$ was entirely unexpected, and provides a novel example of a bridging thallium centre. Despite the formation of **1b** and **2a** as a mixture, this preparation was optimised to produce a useful one-pot synthesis of complex **4b**. The reactions of **4b** with simple donor molecules L (L = PPh_3, Bu^tNC, NC_5H_5) gave the expected products, but the inability of compound **4b** to react with alkynes and alkenes to yield stable adducts is curious, particularly in the light of successful reactions with tungsten– and molybdenum–alkylidyne complexes [3]. The latter reac-

tions may be driven to isolable complexes by virtue of metal–metal bond formation. It seems, however, that **4b** is a reactive species and will yield further interesting chemistry.

4. Experimental section

Solvents were distilled from appropriate drying agents under nitrogen prior to use. Petroleum ether refers to that fraction of boiling point 40–60°C. All reactions were carried out under an atmosphere of dry nitrogen using Schlenk line techniques. Chromatography columns (ca. 15 cm in length and 2 cm in diameter) were packed with silica gel (Aldrich, 70–230 mesh) or alumina (Aldrich, ca. 150 mesh). TLC was performed on preparative UNIPLATES (silica gel G; Analtech). Celite pads for filtration were ca. 3 cm thick. Chemicals were purchased commercially from Aldrich Chemical or Acros, except Tl[*closo*-1,2-Me_2-3,1,2-$TlC_2B_9H_9$] [10] and [$RuBr(CO)_3(\eta^3$-$C_3H_5)$] [11], which were prepared by the literature methods. The NMR spectra reported in Table 3 were recorded at the following frequencies: ^{1}H at 360.13, ^{13}C at 90.56, ^{31}P at 145.78 and ^{11}B at 115.5 MHz.

*4.1. Synthesis of [NEt_4][$Ru_2(\mu$-Tl)$(CO)_4(\eta^5$-7,8-Me_2-7,8-$C_2B_9H_9)_2$] (**2b**)*

A mixture of [$RuBr(CO)_3(\eta^3$-$C_3H_5)$] (1.00 g, 3.26 mmol) and Tl[*closo*-1,2-Me_2-3,1,2-$TlC_2B_9H_9$] (2.00 g, 3.51 mmol) in THF (50 cm^3) was heated to reflux for 4 h. The mixture was cooled to room temperature followed by the addition of [NEt_4]Cl (0.80 g, 4.8 mmol). After stirring for another 1 h, the precipitate was filtered off and the solvent of the red filtrate was removed in vacuo. The residue was dissolved in CH_2Cl_2 (ca. 5 cm^3) and chromatographed on alumina. The complex [$Ru(CO)_3(\eta^5$-7,8-Me_2-7,8-$C_2B_9H_9)$] (**1b**) was removed first by eluting with CH_2Cl_2–petroleum ether (1:1). Further elution with neat CH_2Cl_2 removed a very broad yellow fraction. Yellow microcrystals of [NEt_4][$Ru_2(\mu$-Tl$)(CO)_4(\eta^5$-7,8-Me_2-7,8-$C_2B_9H_9)_2$] (**2b**) (0.53 g) were obtained after the removal of the solvent in vacuo and crystallisation from CH_2Cl_2-petroleum ether (1:2, 15 cm^3).

*4.2. One-pot synthesis of [NEt_4][$RuI(CO)_2(\eta^5$-7,8-Me_2-7,8-$C_2B_9H_9)$] (**3b**)*

A mixture of [$RuBr(CO)_3(\eta^3$-$C_3H_5)$] (0.76 g, 2.48 mmol) and Tl[*closo*-1,2-Me_2-3,1,2-$TlC_2B_9H_9$] (1.51 g, 2.65 mmol) in THF (40 cm^3) was heated to reflux for 4 h. The reaction was monitored by IR spectroscopy. At this stage, the IR spectrum showed that the reaction mixture consisted mainly of [$Ru(CO)_3(\eta^5$-7,8-Me_2-7,8-$C_2B_9H_9)$] (**1b**) and Tl[$Ru_2(\mu$-Tl$)(CO)_4(\eta^5$-7,8-Me_2-7,8-$C_2B_9H_9)_2$] (**2a**) in a ratio of 2:3 respectively. The salt [NEt_4]I (0.69 g, 2.68 mmol) was then added, and the reaction mixture was heated to reflux for a further 2 h. The IR spectrum showed that **1b** had reacted completely to give [NEt_4][$RuI(CO)_2(\eta^5$-7,8-Me_2-7,8-$C_2B_9H_9)$] (**3b**). The mixture was then cooled to 0°C, and I_2 added in portions (0.27 g, 1.06 mmol) until the IR spectrum showed no more compound **2a** was present. The mixture was gradually warmed to room temperature and the suspension was then filtered through Celite. Solvent was removed in vacuo, and the residue was washed with diethyl ether (30 $cm^3 \times 3$) and petroleum ether (20 $cm^3 \times 3$) to give **3b** as a red solid (1.47 g). The product is sufficiently pure for subsequent reactions. However, analytically pure **3b** can be obtained from a CH_2Cl_2 solution layered with petroleum ether to give red crystals.

*4.3. Synthesis of [$Ru(THF)(CO)_2(\eta^5$-7,8-Me_2-7,8-$C_2B_9H_9)$] (**4b**)*

Compound **3b** (0.08 g, 0.14 mmol) in THF (10 cm^3) was treated with $AgBF_4$ (0.03 g, 0.14 mmol). After 5 min, solvent was removed in vacuo. The residue was treated with CH_2Cl_2 (20 cm^3) and the suspension filtered through Celite. The resulting yellow solution of [$Ru(THF)(CO)_2(\eta^5$-7,8-Me_2-7,8-$C_2B_9H_9)$] (**4b**) can be used in situ. Because THF is lost when samples are subjected to extended drying in vacuo, it was not possible to obtain suitable samples of **4b** for microanalysis.

*4.4. Synthesis of [$Ru(NCMe)(CO)_2(\eta^5$-7,8-Me_2-7,8-$C_2B_9H_9)$] (**4c**)*

A similar procedure using **3b** (0.31 g, 0.54 mmol) and $AgBF_4$ (0.11 g, 0.55 mmol) and MeCN (20 cm^3) in place of THF gave yellow microcrystals of [$Ru(NCMe)(CO)_2(\eta^5$-7,8-Me_2-7,8-$C_2B_9H_9)$] (**4c**) (0.15 g) after crystallisation from MeCN–petroleum ether (1:2, 10 cm^3) at −20°C.

*4.5. Synthesis of [$Ru(PPh_3)(CO)_2(\eta^5$-7,8-Me_2-7,8-$C_2B_9H_9)$] (**4d**)*

A yellow solution of **4b** in CH_2Cl_2 (20 cm^3) was generated from **3b** (0.35 g, 0.61 mmol) and $AgBF_4$ (0.12 g, 0.62 mmol), as described above. To this, PPh_3 (0.17 g, 0.65 mmol) was added and the mixture stirred for 10 m. Solvent was reduced in volume in vacuo to ca. 5 cm^3 and the solution chromatographed on silica gel. Elution with CH_2Cl_2–petroleum ether (1:1) removed a yellow fraction. Solvent was then removed in vacuo to leave a yellow oil. Yellow microcrystals of [$Ru(PPh_3)(CO)_2(\eta^5$-7,8-Me_2-7,8-$C_2B_9H_9)$] (**4d**) (0.18 g) were formed upon crystallisation from CH_2Cl_2–petroleum ether (3:7, 15 cm^3).

4.6. Synthesis of [Ru(CNBu^t)(CO)$_2$(η^5-7,8-Me$_2$-7,8-C$_2$B$_9$H$_9$)] (**4e**)

A similar procedure used a solution of **4b** in CH_2Cl_2 (20 cm^3) (generated from **3b** (0.31 g, 0.54 mmol) and $AgBF_4$ (0.11 g, 0.55 mmol), as described above) which was treated with Bu^{t}NC (67 μL, 0.64 mmol). Chromatography on silica gel, followed by crystallisation from CH_2Cl_2–petroleum ether (1:4, 10 cm^3) yielded yellow microcrystals of [Ru(CNBu^t)(CO)$_2$(η^5-7,8-Me$_2$-7,8-C$_2$B$_9$H$_9$)] (**4e**) (0.19 g).

4.7. Synthesis of [Ru(NC$_5$H$_5$)(CO)$_2$(η^5-7,8-Me$_2$-7,8-C$_2$B$_9$H$_9$)] (**4f**)

Using a similar procedure, a solution of **4b** in CH_2Cl_2 (20 cm^3) (generated from **3b** (0.26 g, 0.45 mmol) and $AgBF_4$ (0.09 g, 0.46 mmol), as described above) when treated with pyridine (1 cm^3, 12.4 mmol) gave yellow microcrystals of [Ru(NC$_5$H$_5$)(CO)$_2$(η^5-7,8-Me$_2$-7,8-C$_2$B$_9$H$_9$)] (**4f**).

4.8. Synthesis of [Ru(CO)$_2${η^2,η^5-7,8-Me$_2$-10-C(H)=C(H)SiMe$_3$-7,8-C$_2$B$_9$H$_8$}] (**5a**)

A yellow solution of **4b** in THF (20 cm^3) was generated from **3b** (0.33 g, 0.57 mmol) and $AgBF_4$ (0.12 g, 0.58 mmol). The solvent was removed in vacuo, then CH_2Cl_2 (15 cm^3) added and the suspension filtered through Celite. To the filtrate was added a solution of $Me_3SiC{\equiv}CH$ (82 μL, 0.58 mmol) in CH_2Cl_2 (5 cm^3). The solution was stirred at room temperature for 2 h. The solvent was removed in vacuo and the yellow residue was extracted with CH_2Cl_2–petroleum ether (1:1, 10 cm^3). The extract was then chromatographed on silica gel, eluting with CH_2Cl_2–petroleum ether (1:1). A very broad yellow fraction was collected, which IR and NMR spectroscopy showed to be a complex mixture. Further purification was achieved by preparative TLC with elution by CH_2Cl_2–petroleum ether (1:4). The top yellow band was collected, and extracted with CH_2Cl_2 (30 cm^3). Filtration and removal of solvent in vacuo gave yellow microcrystals of [Ru(CO)$_2${η^2,η^5-7,8-Me$_2$-10-C(H)=C(H)SiMe$_3$-7,8-C$_2$B$_9$H$_8$}] (**5a**) (0.05 g).

4.9. X-ray structural analysis of **2b**

A suitable single-crystal of **2b** for X-ray diffraction was obtained from a THF solution layered with petroleum ether. A low temperature data set for **2b** was collected with the crystal mounted on a glass fiber. Data were collected on a Siemens SMART CCD area-detector 3-circle diffractometer using Mo Kα X-radiation, $\lambda = 0.71073$ Å. Crystallographic parameters are listed in Table 4. For the three settings of ϕ, narrow data 'frames' were collected for 0.3° increments in ω. In all cases, 1321 frames of data were collected affording rather more than a hemisphere of data. The substantial redundancy in data allows empirical absorption corrections to be applied using multiple measurements of equivalent reflections. Data frames were collected for 20 s per frame giving an overall data collection time of ca. 10 h. The data frames were integrated using SAINT [12] and the structure was solved by conventional direct methods. The structure was refined by full-matrix least-squares on all F^2 data using Siemens SHELXTL 5.03 [12], and with anisotropic thermal parameters for all non-hydrogen atoms. All hydrogen atoms were included in calculated positions and allowed to ride on the parent boron or carbon atoms with isotropic thermal parameters ($U_{iso} = 1.2 \times U_{iso\ equivalent}$ of the parent atom except for Me protons where $U_{iso} = 1.3 \times U_{iso\ equivalent}$). The thallium atom Tl(1) lies on a two-fold axis of symmetry. The nitrogen atom N of the $[NEt_4]^+$ cation also sits on a two-fold axis of symmetry, with two ethyl groups located and the remaining two generated by symmetry. Both the ethyl groups located revealed de-

Table 4
Crystallographic data for **2b**

Formula	$C_{20}H_{50}B_{18}NO_4Ru_2Tl$	F(000)	1872
Mol wt	969.70	Crystal dimensions (mm)	0.20 × 0.20 × 0.50
T (K)	173	Crystal colour, shape	Yellow prism
Crystal system	Orthorhombic	Reflections measured	16092
Space group	*Pbcn*	Independent reflections	3246
a (Å)	23.164(2)	2θ range (deg)	4.9 to 50.0
b (Å)	13.780(2)	Refinement method	Full-matrix least-squares on all F^2 data
c (Å)	11.560(6)	Final residuals	$wR_2 = 0.060$[a] ($R_1 = 0.023$)[b]
V (Å^3)	3690(2)	Weighting factors	$a = 0.0292$; $b = 8.2229$[a]
Z	4	Goodness-of-fit on F^2	1.126
D_{calc} (g cm^{-3})	1.746	Final electron density diff features (max/min) (e Å^{-3})	0.95, −0.75
μ(Mo Kα) (mm^{-1})	5.194		

[a]Structure was refined on F_o^2 using all data: $wR_2 = [\Sigma[w(F_o^2 - F_c^2)^2]/\Sigma w(F_o^2)^2]^{1/2}$ where $w^{-1} = [\sigma^2(F_o^2) + (aP)^2 + bP]$ and $P = [\max(F_o^2,0) + 2F_c^2]/3$.
[b]The value in parentheses is given for comparison with refinements based on F_o with a typical threshold of $F_o > 4\sigma(F_o)$ and $R_1 = \Sigma||F_o| - |F_c||/\Sigma|F_o|$ and $w^{-1} = [\sigma^2(F_o) + gF_o^2]$.

Table 5
Atomic positional parameters (fractional coordinates $\times 10^4$) and equivalent isotropic displacement parameters ($Å^2 \times 10^3$) for the atoms of **2b**

Atom	*x*	*y*	*z*	U_{eq}[a]
Tl(1)	5000	9213(1)	2500	20(1)
Ru(1)	6017(1)	8978(1)	1590(1)	20(1)
C(1)	6903(2)	8275(3)	1562(3)	26(1)
C(2)	6673(1)	8469(3)	2923(3)	25(1)
B(3)	6008(2)	7960(3)	3149(3)	24(1)
B(4)	5799(2)	7364(3)	1799(3)	24(1)
B(5)	6391(2)	7630(3)	800(4)	26(1)
B(6)	7027(2)	7059(3)	1365(4)	34(1)
B(7)	7204(2)	7610(4)	2682(4)	35(1)
B(8)	6643(2)	7398(4)	3664(4)	33(1)
B(9)	6112(2)	6697(3)	2964(4)	31(1)
B(10)	6350(2)	6483(3)	1520(4)	32(1)
B(11)	6851(2)	6482(4)	2686(4)	38(1)
C(10)	7341(2)	8951(3)	981(4)	37(1)
C(20)	6903(2)	9324(3)	3627(4)	39(1)
C(3)	6177(2)	10332(3)	1745(4)	40(1)
O(3)	6282(2)	11135(2)	1815(4)	73(1)
C(4)	5690(2)	9216(3)	150(4)	34(1)
O(4)	5488(2)	9314(3)	−755(3)	57(1)
N	5000	6401(4)	−2500	88(3)
C(31)	4473(3)	5829(4)	−2536(5)	63(2)
C(32)	3818(5)	6118(9)	−2797(13)	44(3)
C(33)	4854(4)	7444(6)	−2305(8)	34(2)
C(34)	4760(5)	7479(8)	−987(8)	52(3)
C(32′)	3966(5)	6434(10)	−2388(14)	55(4)
C(33′)	5061(3)	6489(7)	−937(7)	35(2)
C(34′)	5009(4)	5497(8)	−295(9)	47(2)

[a] Equivalent isotropic *U* defined as one-third of the trace of the orthogonalised U_{ij} tensor.

grees of disorder. One ethyl group pivots about the methylene carbon atom C(31) to give methyl positions C(32) and C(32′), whose site occupations were each fixed at 0.5 during refinement. The remaining ethyl group showed disorder of its methylene [C(33) and C(33)′] and its methyl [C(34) and C(34′)] carbon atoms. All four of these positions were refined with fixed site occupancy factors of 0.5. Because of this severe disorder, protons were not assigned to these carbon atoms. All calculations were carried out on Silicon Graphics Iris, Indigo, or Indy computers. Final atomic positional parameters (x, y, z, U_{eq}) for non-hydrogen atoms are listed in Table 5. Atomic coordinates, bond lengths and angles, and thermal parameters have been deposited at the Cambridge Crystallographic Data Centre.

Acknowledgements

We thank the Robert A. Welch Foundation for support (Grant AA-1201) and Dr. Sihai Li for his initial studies on the formation of **1b** in our laboratory.

References

[1] S. Anderson, D.F. Mullica, E.L. Sappenfield, F.G.A. Stone, Organometallics 14 (1995) 3516.
[2] S. Anderson, D.F. Mullica, E.L. Sappenfield, F.G.A. Stone, Organometallics 15 (1995) 1676.
[3] S. Anderson, J.C. Jeffery, Y.-H. Liao, D.F. Mullica, E.L. Sappenfield, F.G.A. Stone, Organometallics 16 (1997) 958.
[4] Y.-H. Liao, D.F. Mullica, E.L. Sappenfield, F.G.A. Stone, Organometallics 15 (1996) 5102.
[5] G.B. Ansell, M.A. Modrick, J.S. Bradley, Acta Crystallogr. C40 (1984) 1315.
[6] A.L. Balch, J.K. Nagle, M.M. Olmstead, P.E. Reedy Jr., J. Am. Chem. Soc. 109 (1987) 4123.
[7] W.R. Hastings, M.C. Baird, Inorg. Chem. 25 (1986) 2913.
[8] N. Masciocchi, M. Moret, P. Cairati, F. Ragaini, A. Sironi, J. Chem. Soc., Dalton Trans., (1993) 471.
[9] P.A. Jelliss, F.G.A. Stone, J. Organomet. Chem. 500 (1995) 307.
[10] J.L. Spencer, M. Green, F.G.A. Stone, J. Chem. Soc., Chem. Commun., (1972) 1178.
[11] G. Sbrana, G. Braca, F. Piacenti, P. Pino, J. Organomet. Chem. 13 (1968) 240.
[12] Siemens X-ray Instruments, Madison, WI, (1995).